Int. J. Chem. Sci.: 14(1), 2016, 103-127
ISSN 0972-768X
www.sadgurupublications.com

CORROSION INHIBITION OF MILD STEEL IN 1.0 M HCl WITH CASTOR OIL EXTRACT AS INHIBITOR

M. OMOTIOMA[*] and O. D. ONUKWULI[a]

Department of Chemical Engineering, Enugu State University of Science and Technology, P.M.B. 01660, ENUGU, NIGERIA
[a]Department of Chemical Engineering, Nnamdi Azikiwe University, AWKA, NIGERIA

ABSTRACT

This work presents the corrosion inhibition of mild steel in 1.0 M HCl with inhibitor of castor oil (*Ricinus communis*) extract. The castor oil leaves extract was characterized using Fourier transform infrared spectroscopy. Thermometric, weight loss (one factor at a time and response surface methods) and potentiodynamic polarization methods were used for the corrosion inhibition study. Spectroscopic analysis of the corrosion product and scanning electron microscopic analysis of the mild steel were also carried out. The analyses of the experimental results revealed that adsorption of the extract on the surface of the mild steel was spontaneous and occurred according to the mechanism of physical adsorption. The castor oil extract (inhibitor) exhibited optimum inhibition efficiency of 85.18%. It inhibited both cathodic and anodic reactions and acted as mixed-type inhibitor. The spectroscopic analysis of castor oil extract and corrosion product showed that asymmetrically stretched N-O at 1477.44 cm^{-1} peak shifted to symmetric stretched N-O at 1292.28 cm^{-1} peak, stretched C≡C at 2434.10 cm^{-1} peak shifted to 2310.66 cm^{-1} and stretched O-H at peak of 3637.64 cm^{-1} shifted to 3575.92 cm^{-1}. The variation of the number and the nature of the shifts indicate that there is synergy among the functional groups of the castor oil extract in the corrosion inhibition process.

Key words: Castor oil, Corrosion inhibition, FT IR, Mild steel.

INTRODUCTION

Mild steel is usually used for structural applications. It is wieldable, which expands its possible applications. It is a medium carbon steel with carbon content of 0.2-0.5%[1]. Besides carbon, steel contains many chemical elements, which are added into iron to form steel of different kinds having various physical properties[2]. Mild steal dissolves in HCl according to the reaction[3]:

$$Fe_{(s)} + 2HCl_{(aq)} \rightarrow FeCl_{2\,(aq)} + H_{2\,(g)} \quad \ldots(1)$$

[*]Author for correspondence; E-mail: omorchem@yahoo.com; Ph.: +2348035539439

Corrosion is seen as the degradation of metal by electrochemical reaction with its environment. Corrosion reaction takes place by two simultaneous reactions: the oxidation of a metal at an anode (a corroded end releasing electron) and the reduction of a substance at the cathode (a protected and receiving electron). For the reaction to occur, the following conditions must exist:

(i) A chemical potential difference must exist between adjacent sites on a metal surface (or between alloys of a different composition),

(ii) An electrolyte must be present to provide solution conductivity and as a source of material to be released at the cathode, and

(iii) As electrical path through the metal or between metals must be available to permit electron flow.

Mild steel is vulnerable to rust. Pickling of steel is an important application of hydrochloric acid. It removes rust or iron oxide scale from iron or steel before subsequent processing. Equation (2) shows HCl as pickling agent for the pickling of carbon steel grades.

$$Fe_2O_3 + Fe + 6\ HCl \rightarrow 3\ FeCl_2 + 3\ H_2O \qquad \ldots(2)$$

Hydrochloric acid is a monoprotic acid; it can ionize only once to give up one H^+ ion in aqueous hydrochloric acid, the H^+ joins with water molecule to form a hydronium ion, H_3O^+.

$$HCl + H_2O \rightarrow H_3O^+ + Cl^- \qquad \ldots(3)$$

The HCl used for pickling, cleaning, and descaling metallic structures often corrode the metals. The adverse effects of the corrosion on the safe, reliable and efficient operation of equipment or structures are often more serious than the simple loss of a mass of metal. There is need for the corrosion control by eco-friendly inhibitors of plant extracts.

Corrosion inhibition of mild steel in HCl medium using cationic surfactant has been examined[4]. The quest for eco-friendly inhibitors suggests the use of plant-derived substances such as extract of castor oil for corrosion control. Studies on medical applications of leaves extract of castor oil have been reported[5,6]. For corrosion inhibition study, extract of castor oil is of great interest owing to its availability and the need to explore its versatile applications. Castor oil is a species of flowering plant in the spurge family, *Euphorbiaceae*. It belongs to a monotypic genus, *Ricinus*, and subtribe, *Ricininae*.

In corrosion inhibition process, some constituents of plant extract (inhibitor) may be adsorbed as protonated or molecular species, with the predominant adsorption mode depending on the prevailing test conditions at any time[7-9]. Thus, there is need to employ test techniques of corrosion inhibition with due consideration to behavioral pattern of the inhibitor.

EXPERIMENTAL

Materials and method

Extraction of the plant extracts

Leaves of castor oil were collected from Akpugo, Enugu state, Nigeria. Leaves of the castor oil were sun dried for three days. The dried leaves were ground to increase the surface area and stored in a closed container. For every of the extraction process, 30 g of each of the ground castor oil leaves were measured and soaked in 1000 mL of ethanol for 48 hrs. At the end of the 48 hrs, each plant mixture was filtered. The filtrate obtained is a mixture of the plant extract and the ethanol. The extract obtained in ethanol solvent was concentrated, distilling off the solvent and evaporate to dryness. The plant extract was weighed and stored for the corrosion inhibition study.

Metals preparation

Sheet of mild steel with composition of P (0.02%), Mn (0.11%), Si (0.02%), S (0.02%), Cu (0.01%), C (0.23%), Ni (0.02), Cr (0.01%) and Fe (99.56%) was cut into coupons (5 cm x 4 cm x 0.1 cm). The coupons were cleaned followed by polishing with emery paper to expose shining polished surface. To remove any oil and organic impurities, the coupons were degreased with acetone and finally washed with distilled water, dried in air and then stored in desiccators. Accurate weight of each coupon was taken using electronic weighing balance and the initial weight was recorded.

FT IR Analysis of the castor oil extract and corrosion product

The mild steel was immersed in the HCl medium in the presence of the castor oil extract. At the end of the corrosion study, the corrosion products in the beakers were collected with the aid of sample bottles. Fourier transform infrared spectrophotometer (SHIMADZU, Model: IR affinity-1; S/N A 2137470136 SI) was used for the determination of the functional groups of the leaves extract of castor oil and corrosion products in the presence of the leaves extract of castor oil. Comparative analysis of various FT IR produced peaks were carried out so as to determine the appropriate functional groups for the corrosion inhibition process.

Thermometric method of the corrosion inhibition study

The measurements were carried using a thermostat set at 30^{o}C for the mild steel in free and inhibited HCl. The temperatures of the system containing the Mild steel and the test solution were recorded regularly until a steady temperature value was obtained. The reaction number (RN) was evaluated using Equation (4)[9,10].

$$RN = \frac{T_m - T_i}{t} \quad \ldots(4)$$

Where T_m and T_i are the maximum and initial temperatures (in ^{o}C), respectively, and t is the time in minutes elapsed to reach T_m.

The inhibitor efficiency was determined using Equation (5)[10].

$$IE\% = (1 - \frac{RN_{add}}{RN_{free}}) \times 100 \quad \ldots(5)$$

Where RN_{free} and RN_{add} are the reaction numbers for the metal dissolution in free and inhibited corrosive medium, respectively.

Weight loss (gravimetric) method of the Corrosion Inhibition Study

Weight loss method using one factor at a time

Considering one factor at a time, the weight loss method was carried out at different temperatures and with various concentrations of the castor oil extract. According to this method, weighed mild steel coupons were separately immersed in 250 mL open beakers containing 200 mL of 1.0 M HCl. Also, mild steel coupons were separately immersed in 250 mL open beakers containing 200 mL of 1.0 M HCl with various concentrations of the castor oil extract.

The variation of weight loss was monitored periodically at various temperatures in the absence and presence of various concentrations of the extract. At the appropriate time, the coupons were taken out, immersed in acetone, scrubbed with a bristle brush under running water, dried and reweighed. The weight loss was calculated as the difference between the initial weight and the weight after the removal of the corrosion product. The experimental readings were recorded. The weight loss (Δw), corrosion rate (CR) and

inhibition efficiency (IE) were determined using the Equations (6), (7) and (8) respectively. The surface coverage was obtained using the following Equation (9)[11].

$$\Delta w = w_i - w_f \quad \ldots(6)$$

$$CR = \frac{w_i - w_f}{At} \quad \ldots(7)$$

$$IE\% = \frac{\omega_0 - \omega_1}{\omega_0} \times 100 \quad \ldots(8)$$

$$\theta = \frac{\omega_0 - \omega_1}{\omega_0} \quad \ldots(9)$$

Where w_i and w_f are the initial and final weight of mild steel samples, respectively; ω_1 and ω_0 are the weight loss values in presence and absence of inhibitor, respectively. A is the total area of the mild steel sample and t is the immersion time.

Effect of temperature on the corrosion rate

Effect of temperature on the corrosion rate was described using Arrhenius equation;

$$CR = A\, e^{-E_\alpha/RT} \quad \ldots(10)$$

Where CR is the corrosion rate of the mild steel, A is the pre-exponential factor, E_a is the activation energy, R is the gas constant.

Equation (10) can be linearized to form Equation (11).

$$\text{Ln (CR)} = \ln A - \left(E_\alpha / R\right)\left(\frac{1}{T}\right) \quad \ldots(11)$$

Considering the corrosion rates of the metal at T_1 and T_2 as CR_1 and CR_2, then Equation (11) can be expressed by Equation (12)[12-14].

$$\ln\left(ER_2 / CR_1\right) = \left(E_\alpha / 2.303R\right)\left(\frac{1}{T_1} - \frac{1}{T_2}\right) \quad \ldots(12)$$

Thermodynamic parameter for the adsorption process.

The heat of adsorption Q_{ads} ($kJmol^{-1}$) was calculated using Equation (13)[13,15].

$$Q_{ads} = 2.303\ R\left[\log\left(\frac{\theta_2}{1-\theta_2}\right) - \log\left(\frac{\theta_1}{1-\theta_1}\right)\right] \times \frac{T_2 . T_1}{T_2 - T_1} \quad \ldots(13)$$

Where R is the gas constant, θ_1 and θ_2 are the degree of surface coverage at temperatures T_1 and T_2, respectively.

Consideration of the adsorption isotherms

The data obtained for the degree of surface coverage were used to test for the applicability of different adsorption isotherms (Langmuir, Frumkin, Temkin and Flory-Huggins isotherms).

Langmuir isotherm

Langmuir isotherm can be expressed by Equation (14)[13,16,17].

$$\frac{C}{\theta} = \frac{1}{K} + C \quad \ldots(14)$$

Where C is the concentration of the inhibitor, K is the adsorption equilibrium constant and θ is the degree of surface coverage. In logarithmic form, Equation (15) can be expressed in Equation (15).

$$\log\ \frac{C}{\theta} = \log C - \log K \quad \ldots(15)$$

Frumkin isotherm

Frumkin adsorption isotherm can be expressed according to Equation (16).

$$\log\left((C) \times \left(\frac{\theta}{1-\theta}\right)\right) = 2.303 \log K + 2\,\alpha\theta \quad \ldots(16)$$

Where K is the adsorption-desorption constant and α is the lateral interaction term describing the interaction in adsorbed layer.

Temkin isotherm

Temkin isotherm can be expressed by Equation (17)[13].

$$\theta = \frac{2.303 \log K}{2\,\alpha} - \frac{2.303 \log C}{2\,\alpha} \quad \ldots(17)$$

Where K is the adsorption equilibrium constant, a is the attractive parameter, θ is the degree of surface coverage, C is the concentration of the inhibitor.

Flory-Huggins isotherm

The Flory-Huggins isotherm can be expressed by Equation (18)[13, 18].

$$\log\left(\frac{\theta}{C}\right) = \log K + x \log(1-\theta) \quad \ldots(18)$$

where x is the size parameter and is a measure of the number of adsorbed water molecules substituted by a given inhibitor molecule.

The free energy of adsorption (ΔG_{ads}) was calculated according to Equation (19)[13,18].

$$\Delta G_{ads} = -2.303\ RT \log(55.5\ K) \quad \ldots(19)$$

Where R is the gas constant, T is temperature, K values obtain from the isotherms (Langmuir, Frumkin, Temkin and Flory-Huggins isotherms) were used to obtain the values of ΔG_{ads} according to Equation (19).

Weight loss method using response surface method

Response surface method in design expert software was used to design the experiment for the weight loss method. Inhibitor concentration, temperature and time were the considered factors while weight loss, corrosion rate and inhibition efficiency were the expected responses of the study. The design matrices for the experiments are shown in Table 1 below.

Table 1: Design matrix for the corrosion inhibition of mild steel in HCl by the castor oil extract

Std.	Run	Factor 1; A: Inhibitor conc.(g/L)	Factor 2; B: Temp. (K)	Factor 3; C: Time (hr)	Response 1; Weight loss (g)	Response 2; corrosion rate (mg/cm^2h)	Response 3; Inhibition efficiency (%)
1	1	0.2	303	8	-	-	-
15	2	0.6	318	16	-	-	-
10	3	1	318	16	-	-	-
9	4	0.2	318	16	-	-	-

Cont…

Std.	Run	Factor 1; A: Inhibitor conc. (g/L)	Factor 2; B: Temp. (K)	Factor 3; C: Time (hr)	Response 1; weight loss (g)	Response 2; corrosion rate (mg/cm^2 hr)	Response 3; Inhibition efficiency (%)
19	5	0.6	318	16	-	-	-
18	6	0.6	318	16	-	-	-
3	7	0.2	333	8	-	-	-
4	8	1	333	8	-	-	-
6	9	1	303	24	-	-	-
7	10	0.2	333	24	-	-	-
13	11	0.6	318	8	-	-	-
8	12	1	333	24	-	-	-
5	13	0.2	303	24	-	-	-
20	14	0.6	318	16	-	-	-
17	15	0.6	318	16	-	-	-
16	16	0.6	318	16	-	-	-
12	17	0.6	333	16	-	-	-
14	18	0.6	318	24	-	-	-
2	19	1	303	8	-	-	-
11	20	0.6	303	16	-	-	-

The RSM was used to analyze the responses. The ANOVA and graphical analyses of the inhibition efficiencies were carried out. The mathematical models in terms of coded and actual factors were obtained. The model in terms of coded factors was used to make predictions about the response for given levels of each factor. The high levels of the factors were coded as +1 and the low levels of the factors were coded as -1. The optimum inhibition parameters were obtained.

Potentiodynamic polarization study

Electrochemical test were conducted using a potentiostat/galvanostat 263 electro-chemical system workstation, with a conventional three-eletrode corrosion cell. A graphite rod and a saturated calomel electrode (SCE) were used as a counter and reference electrodes, respectively. A mild steel specimen fixed in epoxy resin with a surface area of 1 cm^2 exposed to the test solution, served as the working electrode. Electrochemical measurements

were carried out in aerated and unstirred solution at the end of 1800 s of immersion, which allowed the open circuit potential (OCP) to attain steady state. Temperature was fixed at 30 ± 1°C. Potentiodynamic polarization studies were conducted in the potential range ± 250 mV versus corrosion potential at a scan rate of 0.333 mV/s. The inhibition efficiency was determined using Equation (20).

$$IE\ \% = \frac{i_{corr\ (uninh)} - i_{corr\ (inh)}}{i_{corr\ (unmh)}} \times 100 \qquad \ldots(20)$$

Where $i_{corr(uninh)}$ and $i_{corr(inh)}$ are the corrosion current density values without and with inhibitor respectively.

Metal surface study using SEM analysis

Morphological observations of the corroded mild steel samples were carried out using scanning electron microscopy (SEM – Model: Rhenom Prox, Phenom World Eindhoven, Netherlands).

RESULTS AND DISCUSSION

The FT IR spectra of the castor oil leaves extract and corrosion product

The peaks of spectrum of the castor oil leaves extract (Fig. 1) indicate the presence of C=C-H, Ar-H bending out of plane, C-H bending in plane, N-O asymmetric stretch, C=C stretch, C=N stretch, C≡C stretch, C≡N stretch and O-H stretch functional groups in the castor oil extract. The peaks of spectrum of the corrosion product are shown in Fig. 2.

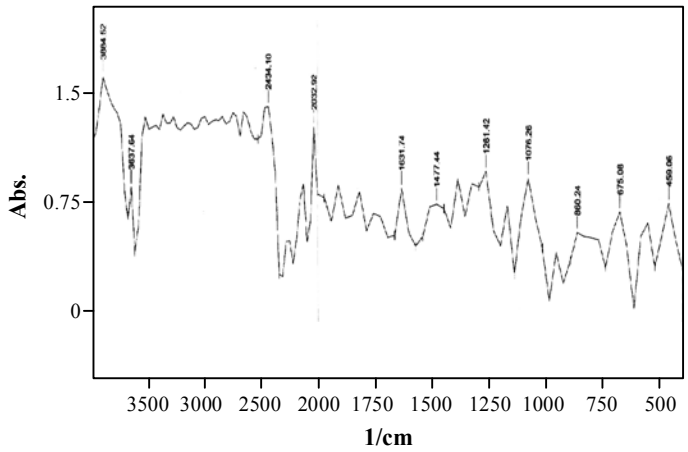

Fig. 1: The FT IR spectrum of the castor oil leaves extract

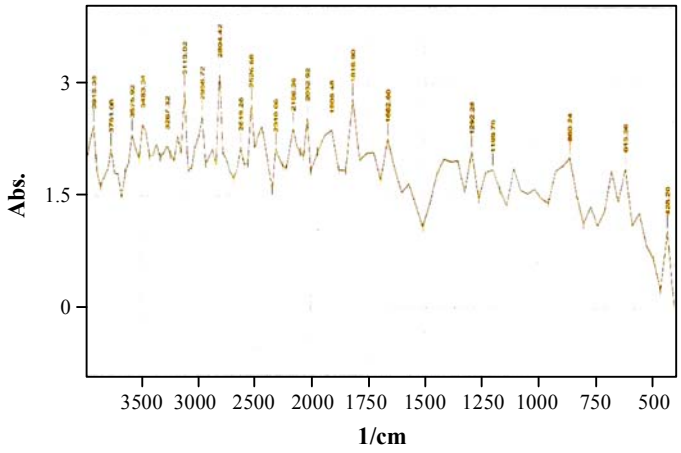

Fig. 2: FT IR spectrum of the corrosion product of mild steel in HCl with castor oil leaves extract

The spectrum of each of the graph shows various peaks in the absorbance versus wave length relationship. The peaks and their corresponding intensities represent the functional group of the plant extract[10,19,20].

Results of the corrosion inhibition as determined by thermometric results

The effect of concentration of the castor oil extract (inhibitor) on the reaction number (RN) and the inhibition efficiency (I.E.) of the mild steal in the HCl medium is presented in Table 2. Increase in concentration of the inhibitor lowers the reaction number. Also, the inhibition efficiency increases with increase in concentration of the inhibitor.

Table 2: Effect of concentration of the extract on the inhibition efficiency, IE (%)

Inhibitor conc. (g/L)	RN	IE (%)
0.0	0.0327	-
0.2	0.0153	53.16
0.4	0.0097	70.35
0.6	0.0061	81.29
0.8	0.0044	86.48
1.0	0.0035	89.38

Results of weight loss method

Results of weight loss method using one factor at a time

The experimental results of weight loss and corrosion rate using one factor at a time are presented Table 3.

Table 3: Data of corrosion inhibition of mild steel in HCl with castor oil leaves extract

Time (hr)	Parameter	0.0 g/L, 303 K	0.2 g/L, 303 K	0.4 g/L, 303 K	0.6 g/L, 303 K	0.8 g/L, 303 K	1.0 g/L, 303 K
8	Weight loss (g)	0.057	0.037	0.03	0.02	0.023	0.017
16		0.1	0.057	0.04	0.027	0.02	0.017
24		0.137	0.067	0.047	0.027	0.02	0.017
8	CR (mg/cm^2 hr)	0.356	0.231	0.188	0.125	0.144	0.106
16		0.313	0.178	0.125	0.084	0.062	0.053
24		0.285	0.140	0.098	0.056	0.042	0.035

Time (hr)	Parameter	0.0 g/L, 318 K	0.2 g/L, 318 K	0.4 g/L, 318 K	0.6 g/L, 318 K	0.8 g/L, 318 K	1.0 g/L, 318 K
8	Weight loss (g)	0.067	0.047	0.04	0.037	0.03	0.027
16		0.113	0.067	0.063	0.043	0.037	0.03
24		0.147	0.077	0.063	0.046	0.04	0.033
8	CR (mg/cm^2 hr)	0.419	0.294	0.25	0.231	0.188	0.169
16		0.353	0.209	0.197	0.134	0.116	0.094
24		0.306	0.160	0.131	0.096	0.083	0.069

Time (hr)	Parameter	0.0 g/L, 333 K	0.2 g/L, 333 K	0.4 g/L, 333 K	0.6 g/L, 333 K	0.8 g/L, 333 K	1.0 g/L, 333 K
8	Weight loss (g)	0.077	0.057	0.05	0.04	0.037	0.037
16		0.14	0.097	0.07	0.06	0.057	0.053
24		0.2	0.12	0.093	0.08	0.07	0.063
8	CR (mg/cm^2 hr)	0.481	0.356	0.313	0.25	0.231	0.231
16		0.438	0.303	0.219	0.187	0.178	0.166
24		0.417	0.25	0.194	0.167	0.146	0.131

In graphical form, Fig. 3 presents the plot of inhibition efficiency versus inhibitor concentration and temperature at various times (in series 1, 2, 3). The inhibition efficiency increases with increase in concentration of the inhibitor (plant extract) but decreases with increase in temperature.

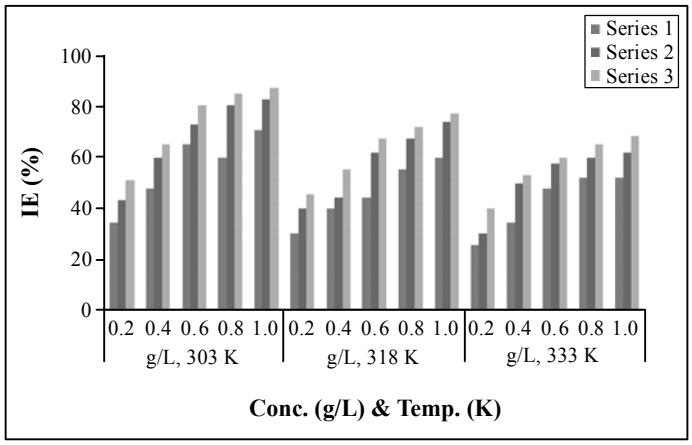

Fig. 3: IE versus concentration and temperature at various times; mild steel in HCl with castor oil leaves extract

The inhibition efficiency and degree of surface coverage of the mild steel in the HCl medium with castor oil extract is presented in Table 4. The inhibition efficiency increases with increase in concentration of the plant extract. But the inhibition efficiency decreases with increase in temperature. Similar trend was noticed in the relationship between the degree of surface coverage and the concentration of the plant extract.

Table 4: The inhibition efficiency (IE) and degree of surface coverage (θ) of mild steel in HCl with castor oil leaves extract

At temperature of 303 K; mild steel area of 5 cm*4 cm; immersion time of 24 hr		
Inhibitor conc. (g/L)	**IE (%)**	**Θ**
0.2	51.09	0.5109
0.4	65.69	0.6569
0.6	80.29	0.8029
0.8	85.40	0.8540
1.0	87.59	0.8759

At temperature of 318 K; mild steel area of 5 cm*4 cm; immersion time of 24 hr		
Inhibitor conc. (g/L)	**IE (%)**	**Θ**
0.2	46.15	0.4615
0.4	55.94	0.5594
0.6	67.83	0.6783
0.8	72.03	0.7203
1.0	76.92	0.7692
At temperature of 333 K; metal area of 5 cm*4 cm; immersion time of 24 hr		
Inhibitor conc. (g/L)	**IE (%)**	**Θ**
0.2	40.00	0.4000
0.4	53.50	0.5350
0.6	60.00	0.6000
0.8	65.00	0.6500
1.0	68.50	0.6850

The activation energy and heat of adsorption

The results of the activation energy and heat of adsorption for the corrosion inhibition of the mild steel in the HCl with castor oil extract are presented in Table 5. In all the cases, the heat of adsorption is negative indicating that the adsorption of the extract on the mild steel surface is exothermic.

Table 5: The activation energy and heat of adsorption for the corrosion inhibition

Conc. of the plant extract (g/L)	Activation energy, E_a (kJ/mol)	Heat of adsorption, Q_{ads} (kJ/mol)
0.2	59.664	-20.069
0.4	70.270	-22.759
0.6	112.433	-44.647
0.8	128.208	-51.271
1.0	135.813	-52.613

Fitting of data into the adsorption Langmuir isotherm

The experimental data were fitted into Langmuir isotherm. As presented in Figure 4, plot of log (C/ θ) versus log (C) shows linear graph.

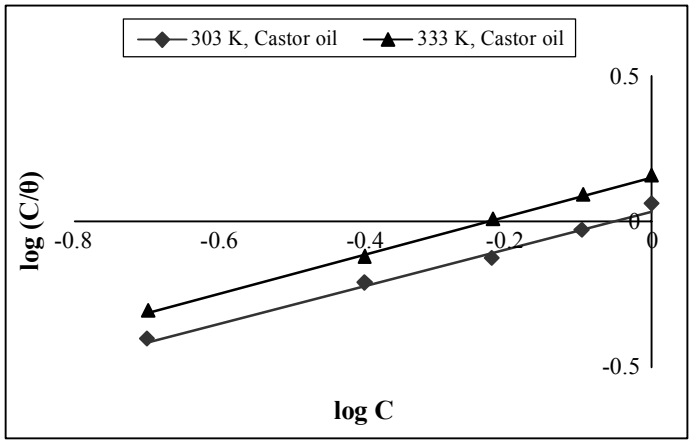

Fig. 4: The ln (C/θ) versus ln C for the corrosion inhibition of mild steel in HCl with castor oil extract

Fitting data into Frumkin isotherm

The experimental data were fitted into Frumkin adsorption isotherm. As presented in Fig. 5, Plot of log ((C)*(θ/(1-θ))) versus θ shows linear graph. The linear relationship indicates that Frumkim isotherm was obeyed.

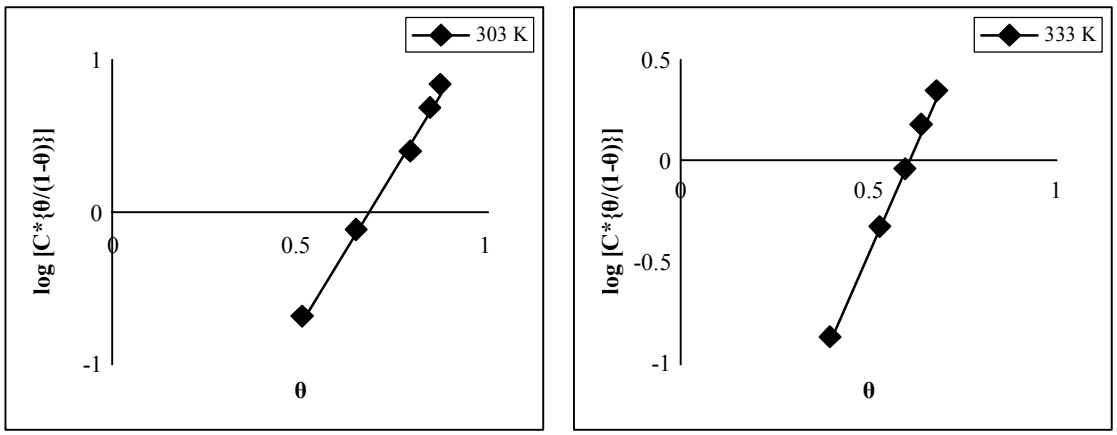

Fig. 5: The log(C*(θ/(1-θ))) versus θ for the corrosion inhibition of mild steel in HCl by castor oil leaves extract

Fitting data into Temkin isotherm

The experimental data were fitted into Temkin isotherm as presented in Fig. 6. The graph of θ versus log C shows linear relationship indicating that Temkin adsorption isotherm was obeyed.

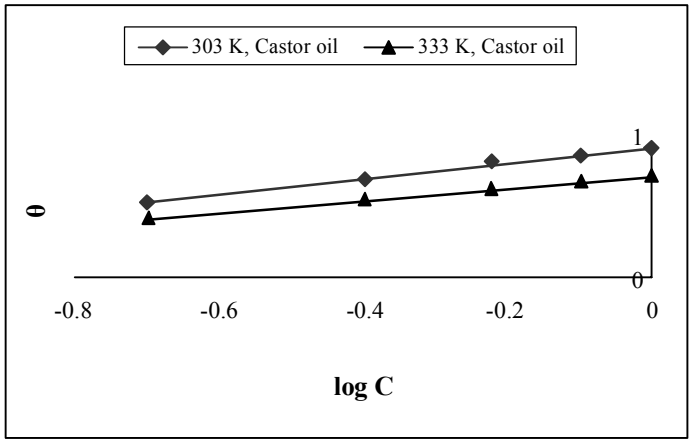

Fig. 6: Plot θ versus ln C for the corrosion inhibition process

Fitting data into Flory-Huggins isotherm

The experimental data were fitted into the Flory-Huggins isotherm as presented in Fig. 7. Plot of log (θ/C) versus ln (1-θ) gave linear relationship. The graph showed that Flory-Huggins isotherm was obeyed.

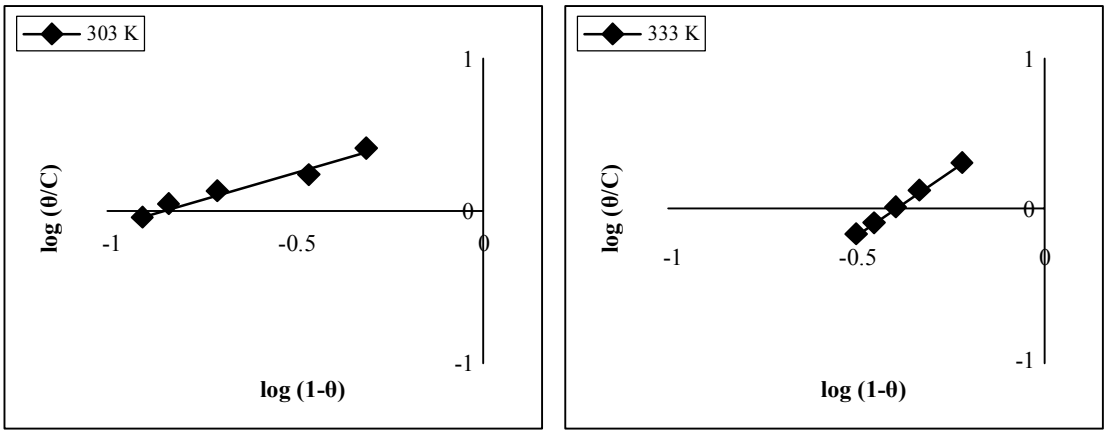

Fig. 7: log (θ/C) versus log (1-θ) for the corrosion inhibition process

The adsorption parameters for the corrosion inhibition

The parameters of the isotherms are presented in Table 6.

Table 6: Adsorption parameters for the corrosion inhibition process

Adsorption isotherm	Temp. (K)	R^2	Log K	ΔG_{ads} (kJ/mol)	Isotherm property	
Langmuir isotherm	303	0.9931	-0.0394	-9.9		
	333	0.9964	-0.1541	-10.0		
Frumkin isotherm	303	0.9907	-1.1964	-3.2	α	2.0116
	333	0.999	-1.1233	-4.0		2.1231
Temkim isotherm	303	0.981	1.623	-19.5	a	-2.086
	333	0.998	1.693	-21.9		-2.829
Flory-huggins Isotherm	303	0.960	0.594	-13.6	x	0.699
	333	0.998	0.675	15.4		1.678

Considering the fitted data to the Langmuir isotherm, the R^2 values are very close to unity, indicating strong adherence to Langmuir adsorption isotherm[21,14].

Results of weight loss method using response surface method (RSM)

The responses of weight loss, corrosion rate and inhibition efficiency to the factors of inhibitor's concentration, temperature and time for the corrosion inhibition of the mild steel in HCl medium with the castor oil extract are presented in Table 7.

Table 7: The RSM result of the corrosion inhibition process

Std.	Run	Factor 1; A: Inhibitor conc. (g/L)	Factor 2; B: Temp. (K)	Factor 3; C: Time (h)	Response 1; Wt. loss (g)	Response 2; Corrosion rate (mg/cm^2 h)	Response 3; Inhibition efficiency (%)
1	1	0.2	303	8	0.037	0.231	35.09
15	2	0.6	318	16	0.043	0.134	61.95
10	3	1	318	16	0.03	0.094	73.45
9	4	0.2	318	16	0.067	0.209	40.71
19	5	0.6	318	16	0.043	0.134	61.95
18	6	0.6	318	16	0.043	0.134	61.95

Cont…

Std.	Run	Factor 1; A: Inhibitor conc. (g/L)	Factor 2; B: Temp. (K)	Factor 3; C: Time (h)	Response 1; Wt. loss (g)	Response 2; Corrosion rate (mg/cm^2 h)	Response 3; Inhibition efficiency (%)
3	7	0.2	333	8	0.057	0.356	25.97
4	8	1	333	8	0.037	0.231	51.95
6	9	1	303	24	0.017	0.035	87.59
7	10	0.2	333	24	0.12	0.25	40
13	11	0.6	318	8	0.037	0.231	44.78
8	12	1	333	24	0.063	0.131	68.5
5	13	0.2	303	24	0.067	0.14	51.09
20	14	0.6	318	16	0.043	0.134	61.95
17	15	0.6	318	16	0.043	0.134	61.95
16	16	0.6	318	16	0.043	0.134	61.95
12	17	0.6	333	16	0.06	0.188	57.14
14	18	0.6	318	24	0.046	0.096	67.83
2	19	1	303	8	0.017	0.106	70.18
11	20	0.6	303	16	0.027	0.084	73

Graphical analysis of the inhibition efficiency, IE (%), as determined using RSM

The analysis of inhibition efficiency of the castor oil extract (inhibitor) of the mild steel in the HCl medium is presented in Figs. 8 below.

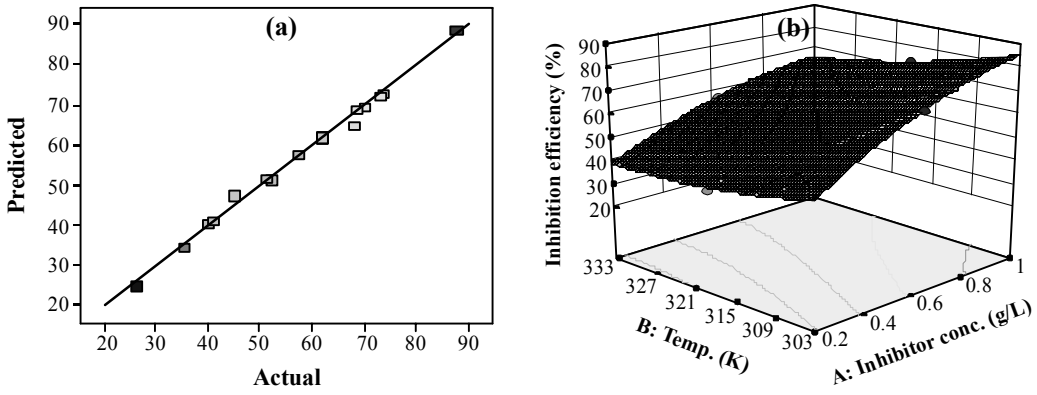

Cont…

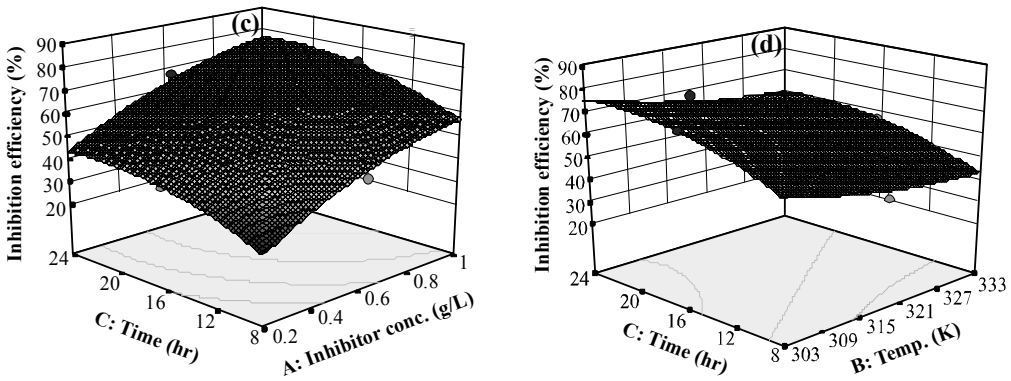

Fig. 8: IE (%) of castor oil leaves extract as corrosion inhibitor of mild steel in HCl (a) Predicted versus actual IE (%) (b) IE (%) versus inhibitor concentration and temperature (c) IE (%) versus inhibitor concentration and time (d) IE (%) versus temperature and time

Predicted versus actual plot is used to test the significance of the model's order. The predicted versus actual plot shows linear graph. The graphs (3-D surface plots) show the relationship between the factors and response (inhibition efficiency) of the designed experiment. Increase in concentration increases the inhibition efficiency. Also, inhibition efficiency reduces as temperature rises.

Mathematical models of the inhibition efficiency

The mathematical models for inhibition efficiency of the castor oil extract as corrosion inhibitor of the mild steel in the HCl medium are shown in Equation (21a) for the coded factors and Equation (21b) for the actual factors. The model shows the relationship among the inhibition efficiency (IE), inhibitor concentration (A), temperature (T) and time (C). The model in terms of coded factors predicts the response for given levels of each factor. The coded model shows the relative impact of the factors.

$$IE = + 62.06 + 15.88*A -7.34*B + 8.70*C -2.14*A*B + 0.49*A*C -0.35*B*C - 5.15*A^2 + 2.84*B^2 -5.92*C^2 \quad \ldots(21a)$$

$$IE = + 1337.86645 + 189.19432 * \text{Inhibitor conc.} -8.26752 * \text{Temperature} + 4.89378 * \text{Time} -0.35646 * \text{Inhibitor conc.} * \text{Temperature} + 0.15352 * \text{Inhibitor conc.} * \text{Time} - 2.94792E\text{-}003 * \text{Temperature} * \text{Time} -32.16193 * \text{Inhibitor conc.}^2 + 0.012640 * \text{Temperature}^2 -0.092514 * \text{Time}^2 \quad \ldots(21b)$$

Considering the significant terms, the models of Equations (21a) ad (21b) reduce to Equations (22a) ad (22b).

IE = + 62.06 + 15.88*A - 7.34*B +8.70*C - 2.14*A*B - 5.15*A^2 + 2.84*B^2 - 5.92*C^2 …(22a)

IE = + 1337.86645 + 189.19432 * Inhibitor conc. - 8.26752 * Temperature + 4.89378 * Time - 0.35646 * Inhibitor conc. * Temperature - 32.16193 * Inhibitor conc.^2 + 0.012640 * Temperature^2 - 0.092514 * Time^2 …(22b)

The analysis of variance (ANOVA) is presented in Table 8 below. From the Table 7, the model F-value of 214.34 implies the model is significant (4.146). There is only a 0.01% chance that an F-value this large could occur due to noise. Values of "Prob> F" less than 0.0500 indicate model terms are significant. In this case A, B, C, AB, A^2, B^2, C^2 are significant model terms. Values greater than 0.1000 indicate the model terms are not significant. The "Pred R-Squared" of 0.9596 is in reasonable agreement with the "Adj R-Squared" of 0.9902; the difference is less than 0.2. "Adeq Precision" measures the signal to noise ratio. A ratio greater than 4 is desirable. The ratio of 61.196 indicates an adequate signal.

Table 8: ANOVA for the corrosion inhibition of mild steel in HCl by castor oil leaves extract

ANOVA for response surface quadratic model						
Analysis of variance Table [Partial sum of squares - Type III]						
Source	Sum of Squares	Df	Mean Square	F Value	p-value Prob > F	
Model	4199.89	9	466.65	214.34	< 0.0001	Significant
A-Inhibitor conc.	2522.06	1	2522.06	1158.43	< 0.0001	
B-Temperature	538.61	1	538.61	247.39	< 0.0001	
C-Time	757.60	1	757.60	347.98	< 0.0001	
AB	36.59	1	36.59	16.81	0.0021	
AC	1.93	1	1.93	0.89	0.3685	
BC	1.00	1	1.00	0.46	0.5131	
A^2	72.82	1	72.82	33.45	0.0002	
B^2	22.24	1	22.24	10.22	0.0095	

Cont…

ANOVA for response surface quadratic model						
Analysis of variance Table [Partial sum of squares - Type III]						
C^2	96.41	1	96.41	44.28	< 0.0001	
Residual	21.77	10	2.18			
Lack of fit	21.77	5	4.35			
Pure error	0.000	5	0.000			
Cor total	4221.66	19				
Std. dev.	1.48		R-Squared		0.9948	
Mean	57.95		Adj R-Squared		0.9902	
C.V. %	2.55		Pred R-Squared		0.9596	
Press	170.50		Adeq Precision		61.196	

From the RSM analysis, optimum inhibition efficiency of 85.18% (at optima inhibitor concentration of 0.94 g/L, temperature of 305.33 K and time of 23.47 hr) was obtained.

The potentiodynamic polarization results

The potentiodynamic polarization curve is presented in Fig. 9. The castor oil extract inhibits both cathodic and anodic reactions and act as mixed-type inhibitors.

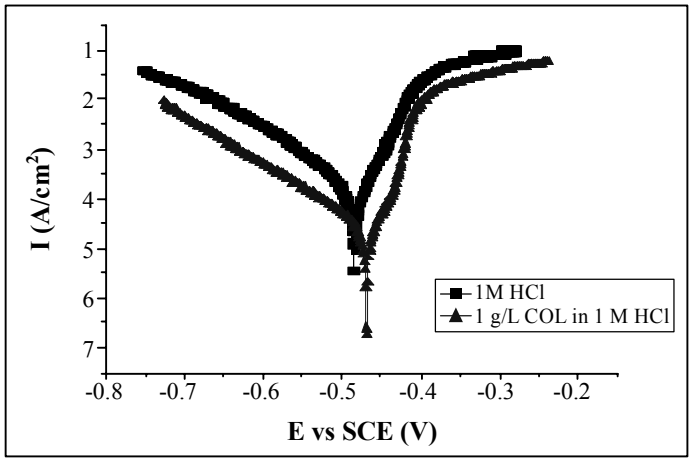

Fig. 9: Potentiodynamic polarization curves for mild steel in HCl in absence and presence of castor oil leaves extract

The parameters from Tafel polarization of the mild steel immersed in the HCl in the absence and presence of the inhibitor (castor oil leaves extract) are shown in Table 9.

Table 9: The parameters from the Tafel polarization

System	E_{corr}	i_{corr}	IE (%)
Mild steel [1 M HCl]:	-504.38	269	
+ 1 g/L castor oil leaves extract	-469	42	84.4

Surface study of the mild seel

The micrographs of the corroded mild steel in the corrosive media in the presence and absence of the castor oil extract are presented in Fig. 10.

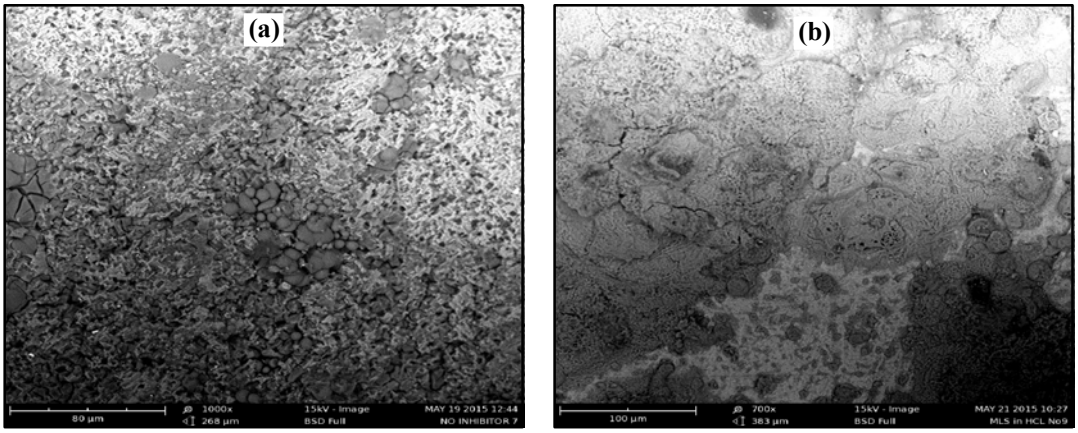

Fig. 10: The micrograph of corroded mild steel surface in HCl (a) without castor oil leaf extract (b) with castor oil leaf extract

The analysis of castor oil extract and corrosion product

Table 10 shows the analysis of castor oil extract and corrosion product of mild steel in HCl (with the castor oil extract). Asymmetrically stretched N-O at 1477.44 cm^{-1} peak shifted to symmetric stretched N-O at 1292.28 cm^{-1} peak, stretched C≡C at 2434.10 cm^{-1} peak shifted to 2310.66 cm^{-1} and stretched O-H at peak of 3637.64 cm^{-1} shifted to 3575.92 cm^{-1}.

Table 10: Peak, intensity and assignment of FT IR of analysis

Castor oil leaves extract			Corrosion product of mild steel in HCl (containing castor oil leaves extract as inhibitor)		
Peak (cm^{-1})	**Intensity**	**Assignment**	**Peak (cm^{-1})**	**Intensity**	**Assignment**
675.08	0.6666	C=C-H, Ar-H bend out of plane	613.36	1.8791	C=C-H, Ar-H bend out of plane
860.24	0.5249	C=C-H, Ar-H bend out of plane	860.24	2.0199	C=C-H, Ar-H bend out of plane
1076.26	0.8975	C-H bend in plane	1199.7	1.8573	C-H bend in plane
1477.44	0.7215	N-O asymmetric stretch	1292.28	2.1001	N-O symmetric stretch
1631.74	0.8330	C=C stretch, C=N stretch	1662.6	2.2599	C=C stretch, C=N stretch
2434.10	1.3988	C≡C stretch, C≡N stretch	2156.36 2310.66	2.4119 2.1299	C≡C stretch, C≡N stretch
3637.64	0.8516	O-H stretch	3483.34 3575.92	2.4463 2.3126	O-H stretch

Further analysis of the results

The inhibition efficiency increases with increase in concentration of the inhibitor (plant extract) but decrease with increase in temperature (Fig. 3 and Table 4). These observations are in agreement with previous studies[22-24]. The data obtained from the degree of surface coverage were used to test for the applicability of different adsorption isotherms; Langmuir, Frumkin, Temkin and Flory-Huggins isotherms. Linear graphs were observed in all the cases. The degree of determination (correlation coefficient, R^2) is close to one (1). The application of Langmuir isotherm to the adsorption of the plant extract on surface of the metal indicates that there is no interaction between the adsorbate and adsorbent. From the Frumkin adsorption parameter, the lateral interaction term (α) gave positive value suggesting attractive behaviour of the inhibitor on the metal surface. From the Temkin adsorption parameter, the attractive parameter value (a) is negative, indicating that repulsion exists in the adsorption layer[14]. The value of the size parameter (x) is positive. This shows that the adsorbed species of the castor oil extract is bulky[13]. The value of free energy of adsorption (ΔG_{ads}) is presented in Table 6. The value of ΔG_{ads} is negative and less than the threshold value of -40 kJ/mol required for chemical adsorption. This is in agreement with the works[13,23]. It is clear that adsorption of the castor oil extract is spontaneous and occurred according to the mechanism of physical adsorption.

Pentiodynamic polarization result provided the insight into the specific effect of the inhibitor on the anodic and cathodic corrosion reactions[7,8,25]. The castor oil extract was found to inhibit the corrosion of the mild steel in the HCl medium, affecting both the cathodic and anodic reactions. The polarization measurements suggest a mixed-inhibition mechanism (Fig. 9). The corrosion process was inhibited by adsorption of the extracted organic matter onto the metal surface. The mechanism of action of the inhibitor depended on the electron density and polarizability of the functional groups present in the molecule.

From Table 10, The shifts in peaks in the FT IR result of the corrosion product, suggest that there is interaction between the mild steel and some molecules of the inhibitor (leaves extract of castor oil). The variation of the number and the nature of the shifts indicate that there is synergy among the functional groups in the corrosion inhibition process.

The electron micrograph of the mild steel revealed that the surface was strongly damaged owing to corrosion in the absence of the inhibitor, but there was little damage on the surface in the presence of inhibitor (Fig. 10). This is attributed to the formation of a good protective film on the mild steel surface[26]. The micrographs have close correlation with the results obtained from the weight loss method.

CONCLUSION

From the analyses of the experimental results, the following conclusions can be drawn:

- Increase in inhibitor concentration increases the inhibition efficiency.
- Inhibition efficiency is concentration, temperature and time dependent.
- Adsorption of the extract on the surfaces of mild steel was spontaneous and occurred according to the mechanism of physical adsorption.
- Optimum inhibition efficiency of 85.18% (at optima inhibitor concentration of 0.94 g/L, temperature of 305.33 K and time of 23.47 hr) of the castor oil extract (inhibitor) was achieved.
- The castor oil extract inhibited both cathodic and anodic reactions and acted as mixed-type inhibitor.
- The variation of the number and the nature of the shifts of the extract's functional groups indicate that there was synergy among the functional groups in the corrosion inhibition process.

REFERENCES

1. O. P. Aggarwal, Engineering Chemistry, 3rd Ed., Kahanna Publishers, New Delhi (2010) pp. 718-797.
2. M. M. Uppal and S. C. Bhatia, Engineering Chemistry (Chemical Technology), 7th Ed., Khanna Publishers, New Delhi (2009) pp. 269-308.
3. A. O. Yuce and G. Kardas, Corrosion Sci., **58**, 86-94 (2012).
4. B. S. Prathibha, P. Kotteeswaran, V. R. Bheema, IOSR J. Appl. Chem. (IOSR JAC), **2(1)**, 45-53 (2012).
5. P. Kalaiselvi, B. Anuradha and C. S. Parameswari, Biomedicine, **23(1-2)**, 95-105 (2003).
6. O. I. Oyewole, A. A. Owoseni and E. O. Faboro, J. Medic. Plant Res., **4(19)**, 2004-2008 (2010).
7. E. E. Oguzie, C. K. Enenebeaku, C. O. Akalezi, S. C., Okoro, A. A. Ayuk and E. N. Ejike, J. Colloid Interface Sci., **349**, 283-292 (2010).
8. M. M. Ihebrodike, M. C. Nwandu, B. O. Kelechukwu, A. N. Lebe, A. C. Maduabuchi, F. C. Eze and E. E. Oguzie, J. Mater. Sci., **47**, 2559-2572 (2011).
9. E. M. Mabrouk, H. Shokry and K. M. Abu Al- Naja, Chem. Met. Alloys, **4**, 98-106 (2011).
10. N. O. Eddy, B. I. Ita, S. N. Dodo and E. D. Paul, Green Chemistry Letters and Reviews, **5(1)**, 43-53 (2012).
11. N. Nagm, N. G. Kandile, E. A. Badr and M. A. Mohammed, Corrosion Science, **65**, 94-103 (2012).
12. L. Octave, Chemical Reaction Engineering, 3rd Ed., John Wily and Sons, New York (2003).
13. J. T. Nwabanne and V. N. Okafor, J. Emerg. Trends Eng. Appl. Sci., **2(4)**, 619-625 (2011).
14. L. A. Nnanna, I. O. Owate, O. C. Nwadiuko, N. D. Ekekwe and W. J. Oji, Int. J. Mater. Chem., **3(1)**, 10-16 (2013).
15. K. Orubite-Okorosaye and N. C. Oforka, J. Appl. Sc. Environ. Mgt., **8(1)**, 57-61 (2004).
16. X. Li and S. Deng, Corrosion Science **65**, 299-308 (2012).

17. N. S. Patel, S. Jauhariand, G. N. Mehta, S. S., Al-Deyeb, I. Warad and B. Hammouti, Int. J. Electrochem. Sci., **8**, 2635-2655 (2013).

18. I. J. Alinno and P. M. Ejikeme, Ame. Chem. Sci. J., **2(4)**, 122-135 (2012).

19. B. S. Furniss, A. J. Hannaford, P. W. G. Smith and A. R. Tatchell, Vogel's Textbook of Practical Organic Chemistry, 5th Ed., Longman Group, UK (1989) pp. 1412-1422.

20. D. Skoog, D. West, J. Holler and S. Crouch, Fundamentals of Analytical Chemistry, 8th Ed., India (2004).

21. V. G. Vasudha and P. K. Shanmuga, Res. J. Chem. Sci., **3(1)**, 21-26 (2013).

22. E. El Ouariachi, J. Paolini, M. Bouklah, A. Elidrissi, A. Bouyanzer, B. Hammouti, J. M. Desjobert and J. Costa, Acta Metal. Sin. (Engl. Lett.), **23(1)**, 13-20 (2010).

23. O. M. Ndibe, M. C. Menkiti, M. N. C. Ijomah and O. D. Onukwuli, Electronic J. Environ. Agricul. Food Chem., **10(9)**, 2847-2860 (2011).

24. M. Abdulwahab, A. Kasim, K. A. Bello and J. O. Gaminana, Adv. Mater. Res., **367**, 319-325 (2012).

25. V. V. Torres, R. S. Amado, F. Camila, T. L. Fernandez, A. S. R. Carlos, A. G. Torres, and D. Elian, Corrosion Sci., **53**, 2385-2392 (2011).

26. C. A. Loto and A. P. I. Popoola, Canadian J. Pure Appl. Sci., **6**(2), 1973-1980 (2012).

Revised : 03.12.2015 *Accepted : 04.12.2015*